



CFD Simulation Using ANSYS FLUENT of Jet Nozzle of Ethanol at Temperature of 360 K

Zurita Ismail¹, Saleha Maarof¹, Mohamed Faris Laham¹, Kai Xin Siah², Muhammad Rezal Kamel Ariffin¹, Nizam Tamchek^{1,2,*}

¹ Institute for Mathematical Research, Universiti Putra Malaysia, 43400 Serdang, Selangor, Malaysia

² Department of Physics, Faculty of Science, Universiti Putra Malaysia, 43400 Serdang, Selangor, Malaysia

ARTICLE INFO

Article history:

Received 15 February 2022

Received in revised form 13 May 2022

Accepted 16 May 2022

Available online 12 June 2022

Keywords:

CFD; elevated temperature; thermal energy; ethanol; spray nozzle

ABSTRACT

Spray coating technology is an advanced manufacturing process to break the liquid down into small droplets and disperse these droplets uniformly on the target substrate. The nozzle used in this fabrication process rapidly disintegrates the liquid jet at a direction of motion governed mainly by the prevailing airflow pattern in the spray region environment. According to Navier–Stokes energy equation, the fluid and environmental temperature capable of supplying additional energy to the droplet imparted the ejected liquid jet from the nozzles. With a view to understanding the liquid droplet behaviour at elevated temperatures, this study investigates the jet velocity, pressure, and temperature of ethanol at its evaporation temperature of 360 K using commercial CFD software (ANSYS FLUENT 2020). A numerical simulation of a simple nozzle system with a cone angle of 56° and an outlet radius of 0.1966 mm was modelled at 1 bar inlet pressure to study the effect of the environment temperature on the liquid jet. The result from the temperature profile showed that the liquid jet exhibited turbulence or a swirling effect at elevated temperature as the liquid absorbed thermal energy. The liquid jet temperature increased to the maximum temperature of +3K at a liquid jet distance of 10 cm when compared with normal environment temperature. This numerical study showed that environmental conditions such as temperature can impact the liquid jet quality and properties, which are difficult to observe during experimental work. It is expected that the finding from this work would benefit the industries, leading to better spray nozzle design for future coating applications.

1. Introduction

Computational fluid dynamics (CFD) is the numerical study of fluid dynamic problems underflows. CFD development allows scientists and engineers to understand complex fluid phenomena in many applications such as fluid flow in spray, pipe, vehicles, surface, pump, or ventilation systems [1]. The fluid dynamics of spray involved several topics from evaporation, atomization, combustion and freezing. Zheng *et al.*, [2] investigated the dynamic process of single splat formation for optimizing

* Corresponding author.

E-mail address: nizamtam@upm.edu.my

<https://doi.org/10.37934/arfmts.96.1.168178>

the plasma spraying process. They have developed a 3D model consisting of heat transfer and phase change by CFD simulation to understand the impact, flattening and solidification of a molten droplet on a solid substrate. Alhulaifi *et al.*, [3] performed a CFD numerical investigation for various nozzle geometries and flow conditions to produce successful coating adhesion on a metal substrate.

Understanding the physics of fluid dynamics and applying it to real-world problems can permit the development of newly emerging technology and ecosystems as (as essential) will benefit and increase productivity. The spray technologies have been utilized in the recent development of a family of carbon such as carbon nanotube (CNT) and graphene by using carbon sources, namely ethanol, palm oil and castor oil which have low hydrogen contents. The technique has successfully fabricated a multi-wall carbon tube with large yields at varying diameters of 20-60 nm and large-area single-layer graphene with coverage up to 97% of the measured area size of 6400 μm^2 [4-6].

Development of new carbon material such as CNT, graphene oxide (GO) and reduced-GO (RGO) for new applications such as sensors, electronic devices, superconductors, catalysts, etc. have been widely investigated due to their high thermal and chemical stability, high aspect ratio and unique electronic properties, see studies by Zhang and Nicolosi [7], Szuromi [8], and Zhu *et al.*, [9]. The fabrication methods used to form a film or layer on the glass or silicon substrate of these unique materials were chemical vapor deposition (CVD), spray coating, sputtering, or dipping techniques. Salleh *et al.*, [10] successfully grow dense and high-quality carbon nanostructure on Ni (nickel) layer by using CVD method. On the other hand, in 2019, Firdaus *et al.*, [11] has continuously produced CNT by using the same method in a rotary reactor. Furthermore, Hussin *et al.*, [12] has fabricated and characterized graphene on silicon substrate by using spray coating technique for advanced power electronic design.

Spray coating processes are well known for their advantages to yield a high production rate with good uniformity because of simplicity and low cost. Application such as electronics and chemical catalysts with required large surface interaction areas will benefit these fabrication routes. However, optimizing the spray processes can be challenging since the chaotic nature of millions of high-velocity spray droplets ejected from the nozzles that concurrent continuously with the spray environment and the final target substrates [13]. Alternatively, second to the CFD approach is a preference means to determine the optimal parameters of the spray process [14].

There are several models of fluid instability during spray processes such Kelvin-Helmholtz and Rayleigh-Taylor that predict the breakup of the liquid. The fluid breakage better known as atomization reduce the fluid internal energy causing a temperature and pressure drop along the path of the ejected droplets. In isolated chamber system such as combustion chamber, the deviation of fuel temperature and pressure led to reduction of engine performance and increased the toxic emission [15].

Inspired by these problems, a numerical study of the ethanol spray process for the development of CNT based material using CFD was conducted using commercially available software ANSYS Fluent 2020. The ethanol liquid was ejected from the nozzle at two different environment temperatures of 300 K and 360 K. Ethanol have low density and viscosity at this temperature range [15]. At 360 K, the ethanol will start to evaporate, which allows us to understand the liquid droplet and vapor mixture of the ejected jet [16]. This work comprised a numerical method, the result of velocity, pressure, and temperature of the jet and finally, the thermal conductivity of the ethanol vapor. From the result of this work, the environment temperature of 360 K has affected the velocity and temperature of the jet, thus reducing the thermal conductivity of the jet at the outlet end of the nozzles. Further down from the nozzles, the velocity and momentum of the jet vary slightly due to the thermal heat of the environment.

2. Methodology

In this work, CFD commercial code ANSYS FLUENT 2020 have been used. Generally, the simulation in ANSYS FLUENT involves three main stages: pre-processing, solver, and post-processing. The design of the nozzle used in this study is only focused on the spray nozzle, substrate, and environment. Figure 1 shows the overall simulation and the analysis flow chart, while Figure 2 shows the schematic diagram of the cross-sectional of the spray nozzle. The nozzle cone angle is 56° , with an outlet radius of 0.1966 mm.

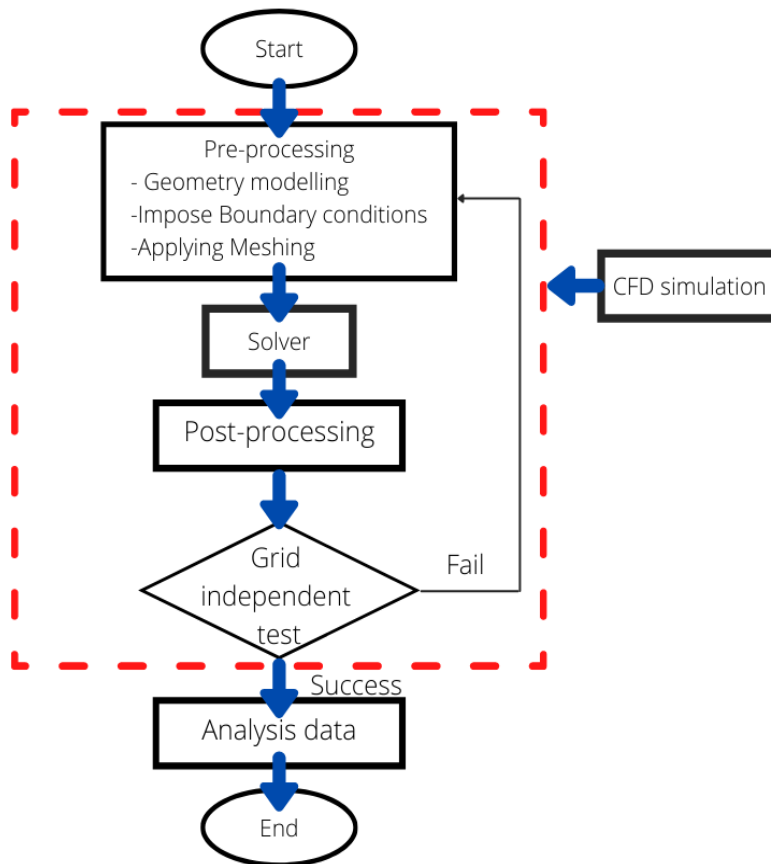


Fig. 1. Modelling flowchart in ANSYS FLUENT

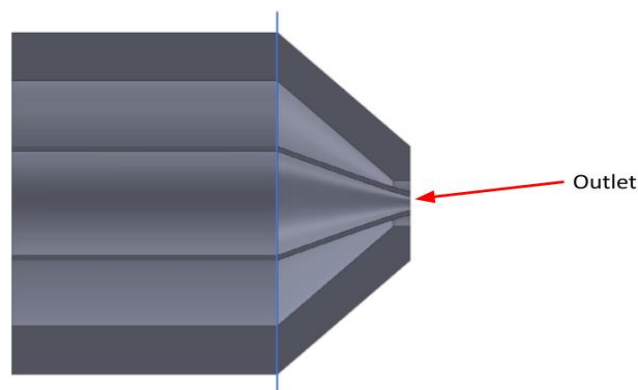


Fig. 2. The schematic diagram of the cross-sectional spray nozzle

For the geometry model, a 2D ANSYS workbench was used, and a 2D planar body is considered in this work. Numerical simulations were carried out on a 2D axisymmetric mesh with quadrilaterals shape and dimensions of 120 mm × 25mm. The quality of the mesh is controlled by the skewness value, 0.9 with a high smoothing condition. The computational domain is divided into seven subdomains, as shown in Figure 3.

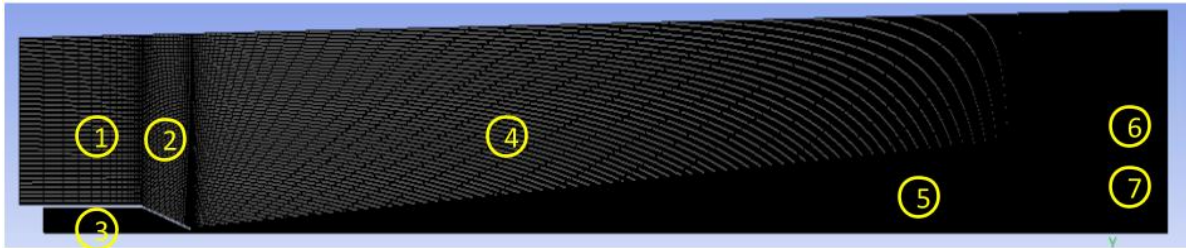


Fig. 3. Mesh modelling with seven subdomains

The total number of cells, 19550 and total binary node, 19896 have been used. Table 1 listed the total area of each section in the domain.

Table 1

The surface area of the mesh

Domain	Surface area (mm ²)
1	189.18
2	81.589
3	28.311
4	1522.2
5	171.74
6	160.83
7	38.098

From the seven domains, subdomains 1, 2 and 4 is the environment or the farfield with temperature parameters, 300 K and 360 K. Subdomain 3 is the spray nozzle with air and ethanol as the solvent, and the injected parameter condition is incompressible. This subdomain is divided into four functions, namely inlet, outlet, wall and axis. The inlet nozzle is known as the convergent section, and the outlet nozzle is known as the divergent section. The significance of the convergent-divergent area is to convert from the potential energy inside the nozzle into kinetic energy before the solvent is coated on the substrate. Subdomain 6 and 7 is the location of the substrate.

Navier–Stokes energy equation was adopted in the model of the simulation. The calculation was coupled with pressure-velocity coupling with a full implicit 2nd order gradient-, pressure-, momentum- and energy-time scheme together with 2nd order spatial discretisation scheme. For viscous models, laminar flow is used due to no viscosity effect during incompressible flow of the fluid. Table 2 shows the boundary condition setting that has been applied in the ANSYS FLUENT to conduct the simulation.

Table 2
 The boundary conditions used in ANSYS FLUENT

Solver	2 D axisymmetric Steady time Velocity combination	Density-based (compressible) Absolute
Model	Viscous Energy equation	Laminar On
Material (Fluid)	Air Ethanol Ideal gas Viscosity by Sutherland law	
Domain/ Boundary Condition	Inlet Outlet Wall Farfield/environment	Pressure inlet: 1 bar Temperature: 300K Pressure outlet: 1 bar Temperature: 300 K Wall Temperature: 300 K and 360 K
Solution initialization	Standard	From Inlet
Reference value	From inlet (fluid surface body)	

In order to improve the calculation accuracy, a high-resolution orthogonal mesh has been used for the entire domain. The simulation was done on AMD Ryzen 5 3600 with 64 GB memory. The test conditions of the work are namely, ethanol solvent injected at 1 bar and the ambient temperature of 300K and 360K.

3. Results and Discussion

Figure 4 shows the temperature contour profile of the air's jet when the environment temperature is 300 K in Figure 4(a) and 360 K in Figure 4(b). As indicated by the temperature colour profile from Figure 4(a), the injected air is kept at the same temperature of 300 K when the jet of the air passes through the space. Compared to Figure 4(b), when the air is ejected from the outlet of the nozzle, no distortion or turbulence effect is observed at the beginning. When the jet of the air passed through space, the temperature of the jet was found to increase at a steady state but just a few degrees (≈ 4 K). The observed temperature gradient at the wall of the nozzle is due to the heat conduction of the nozzle material made from aluminium to the environment producing a region of swirling flow as the cool air from the nozzle inlet is denser than the hot air of the environment.

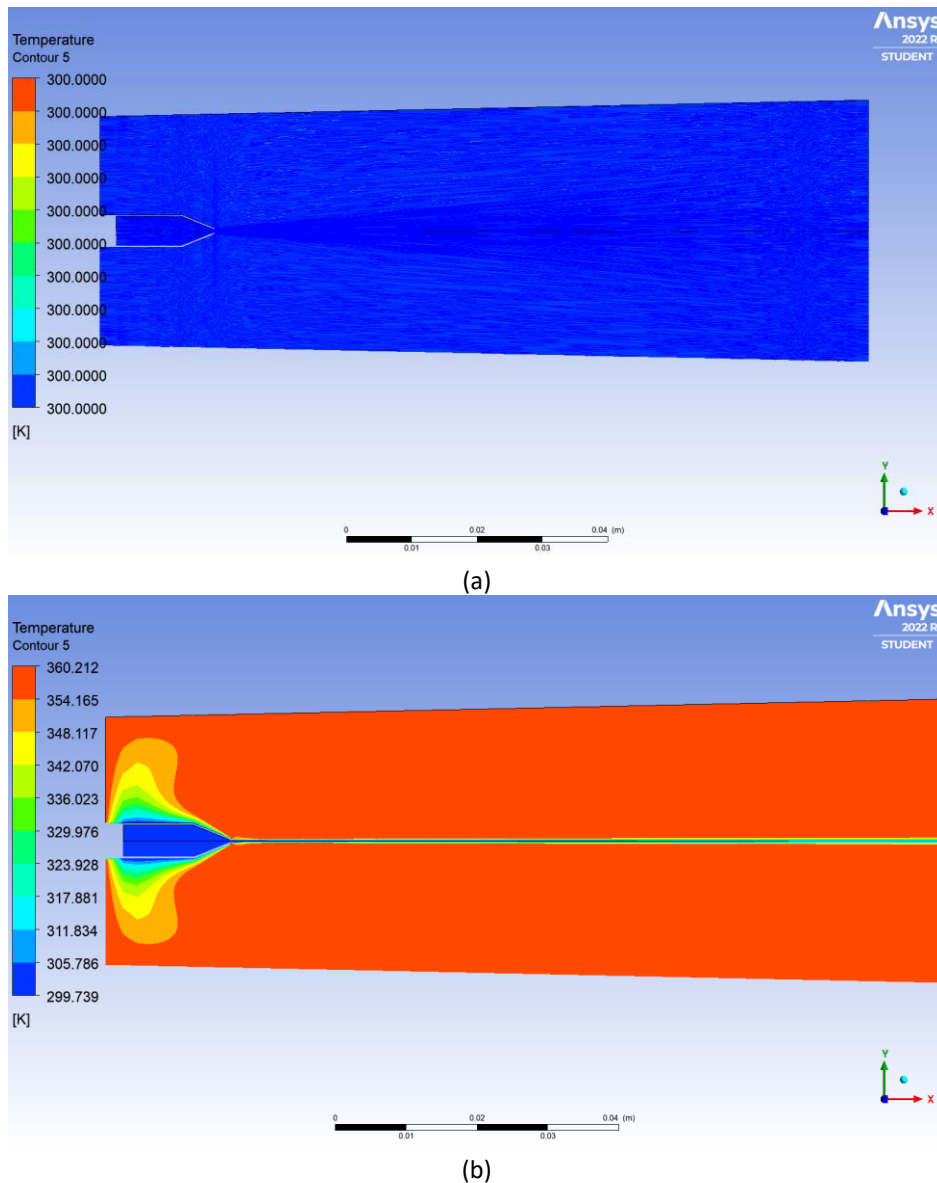


Fig. 4. The temperature profile using air of (a) 300 K and (b) 360 K environment temperature

Figure 5 shows the temperature profile of the simulation using ethanol as the source at 300 K in Figure 5(a) and 360 K in Figure 5(b). The injected air is kept at the same temperature of 300 K. When the environment temperature is 300 K, the temperature of the ejected jet displays no significant difference than a jet of air in Figure 5(a), as there are no temperature gradients across the space of the simulation. Compared to the environment temperature of 360 K, the temperature profile exposed several patterns from the beginning of the fluid inlet to the location of the substrate. There are considerable temperature differences observed at the nozzle outlet as the fluid temperature is cooler at this side. As it travels across space, the temperature of the fluid jet gains to about a maximum of 3 K to the end of the space as it absorbs the heat energy from the environment as shown in Figure 6 creating a large fluid to droplet breakage at distance about 2.4 cm from nozzle outlet. This increased the spray penetration length to almost 6 cm from the nozzle outlet. The spray cone angle beyond the nozzle outlet where the ethanol droplets concentration is higher was found widen to about 40° compared to Figure 4(b). This indicated the turbulent dispersion of ethanol droplet in higher environment temperature.

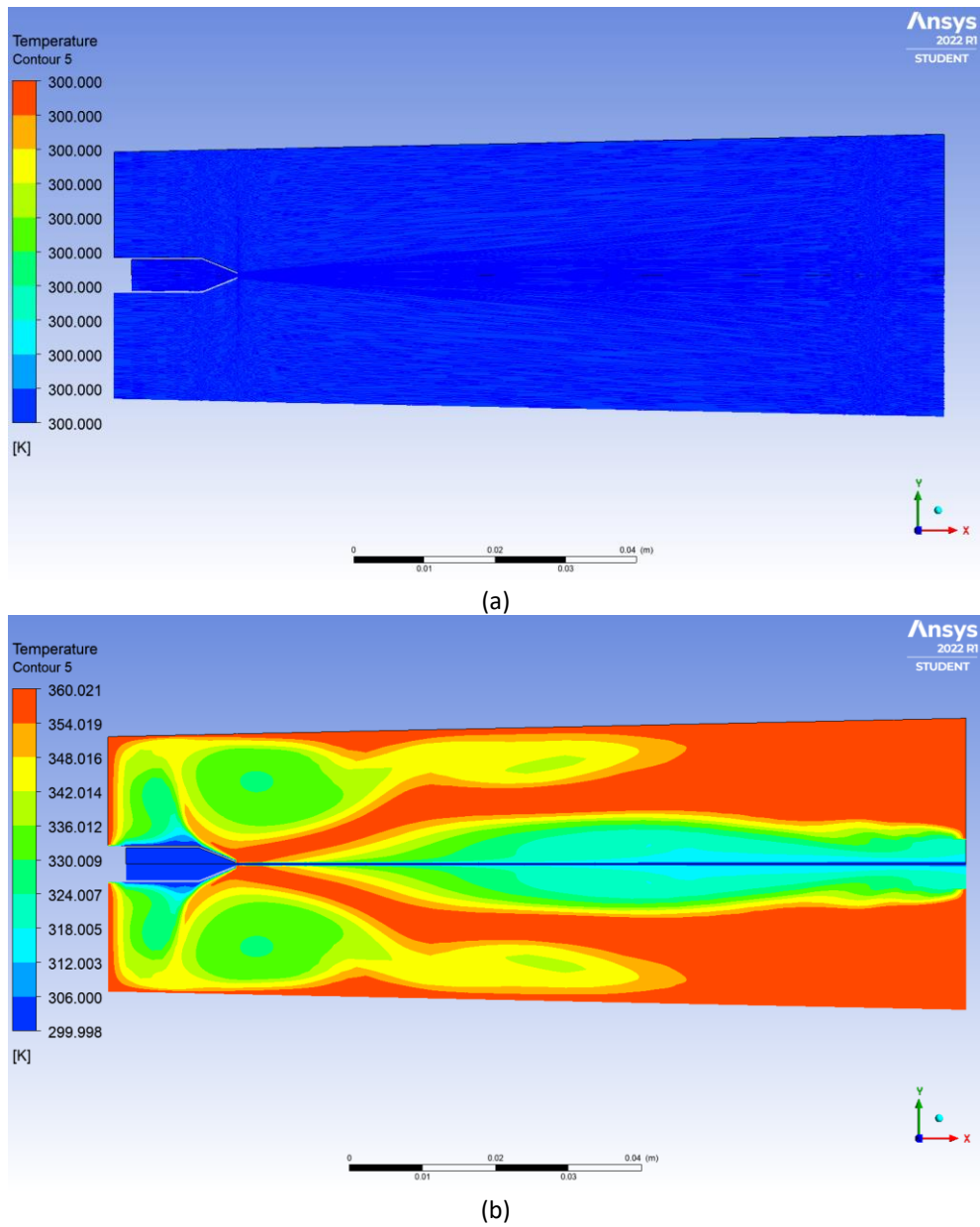


Fig. 5. The temperature profile using ethanol at (a) 300 K and (b) 360 K environment temperature

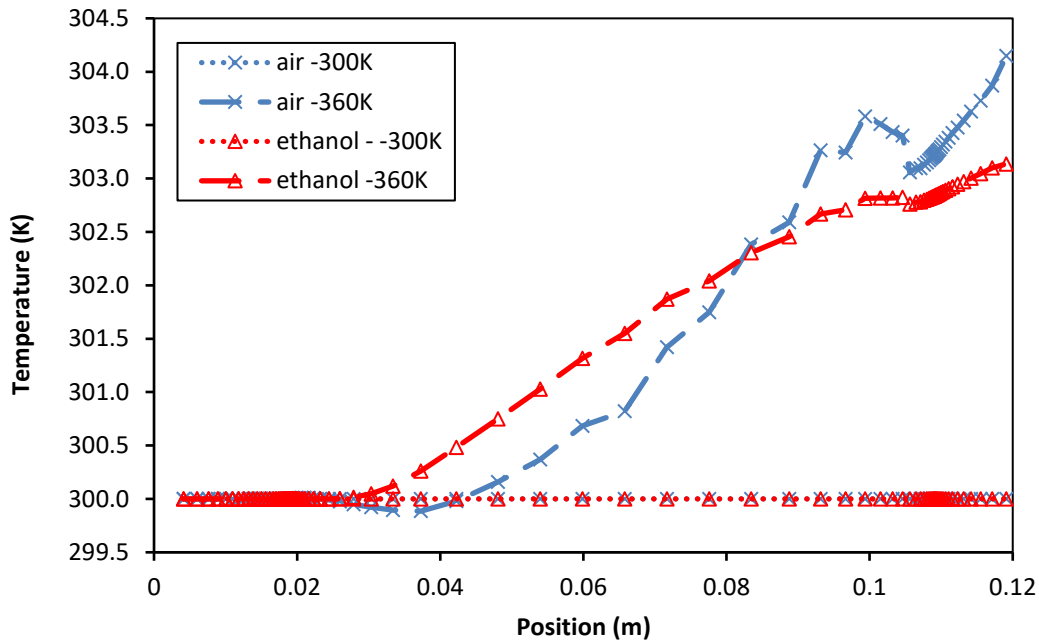


Fig. 6. Temperature as the function of spray position of the air and ethanol at 300K and 360K

Figure 7 shows the pressure of the ejected jet air and ethanol from the nozzle for 300 K and 360 K. The source pressure of the jet is 100k Pa (1 bar). When the jet discharged from the nozzle, it lost its energy to space. The ejected air and ethanol jet at 300K continued at 2800 Pa with a small fluctuation at 0.1 m and beyond as it travelled through space. It indicated the formation of backflow of the ejected ethanol's jet when the pressure is fluctuated, which displayed less back-flow due to high momentum since it has a higher mass than air. For the environmental temperature of 360K, greater pressure fluctuations were observed almost steady to environment pressure with higher backflow. It is because hot air is much lighter than cool jets (mixture of air and ethanol vapour).

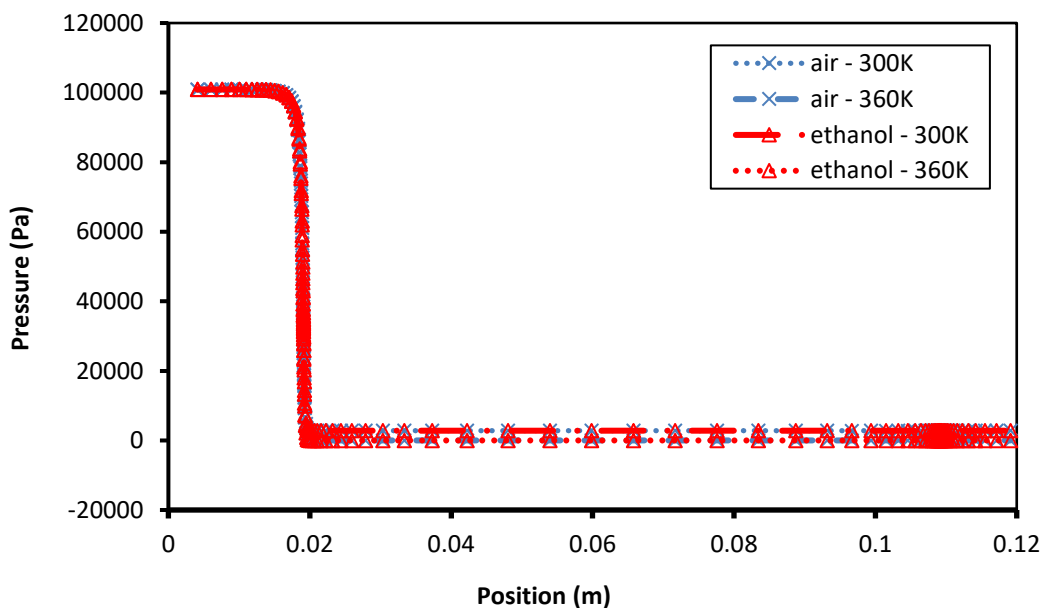


Fig. 7. The pressure of the ejected air and ethanol at 300K and 360K

Figure 8 shows the velocity of the air and ethanol ejected out of the nozzle. The magnitude of the velocity for both 300 K and 360 K was almost the same, but it was found that velocity of the air jet loss was a bit greater as it travelled across space. The momentums of the air jet were lesser than ethanol thus received more velocity variation. From the result, the air jet has a higher velocity than ethanol as the drag experienced by the ethanol droplets in the environment is much higher than the air. This result indicated that the droplets velocity / kinetic energy depends on the thermal energy of the environment. A comparative numerical observation from Jumadi *et al.*, [17] demonstrated the velocity of the gasoline droplets reduced accordingly with environment pressure primarily due to drag that restrict the droplet from travelling in much faster rate and distances.

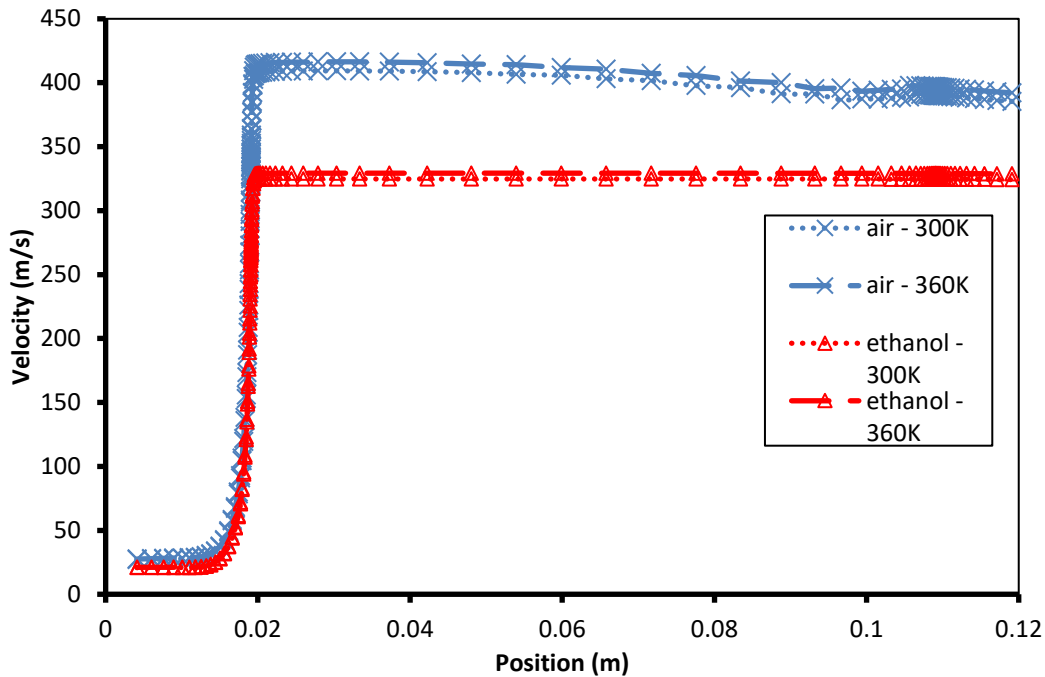


Fig. 8. The velocity of the ejected air and ethanol at 300 K and 360 K

For analysing the effect of environment temperature, the mass of the fluids used in the simulation should be considered an important parameter affecting the fluid flow behaviours. Generally, when the mass of the fluids is heavy, the temperature perturbation is higher, and the velocity of the fluid reaching the substrate will decrease further [18]. This situation will lead to turbulence or a swirling effect as it passes through space [19].

4. Conclusion

Simulation study on spray coating model is investigated with the help of software ANSYS FLUENT 2020. Simulation was done on two different material, ethanol and air at two different environment temperature. The fluid flow properties of the ethanol spray system such as fluid breakage length, spray angle and penetration length were about 6, 40° and 2.4 cm respectively. The velocity, temperature and pressure of the droplet revealed the environment temperature and type of fluid affect the formation of droplet in spray system. The momentum and kinetic energy of the droplet have been discussed to explain the findings. The significant results of this study can be summarized as follows

- i. By increasing the environment temperature, a significant temperature difference can be observed when ethanol was ejected and evaporated at the outlet of the nozzle.
- ii. When the fluid passes the space, the velocity and the momentum of the jet with heavier mass vary slightly due to the thermal heat of the environment.

Acknowledgements

This research was supported by Ministry of Higher Education of Malaysia (MOHE) through Fundamental Research Grant Scheme (FRGS) with reference code, FRGS/1/2019/STG07/UPM/02/9 and Geran Putra (GP-IPM/2021/9703700) funded by Universiti Putra Malaysia.

References

- [1] Mansor, Mohd Radzi Abu, and Zambri Harun. "F1 in SCHOOLS competition to promote STEM: Aerodynamic investigation of miniature F1 in SCHOOLS car." In *2017 7th World Engineering Education Forum (WEEF)*, pp. 708-712. IEEE, 2017.
- [2] Zheng, Y. Z., Q. Li, Z. H. Zheng, J. F. Zhu, and P. L. Cao. "Modeling the impact, flattening and solidification of a molten droplet on a solid substrate during plasma spraying." *Applied Surface Science* 317 (2014): 526-533. <https://doi.org/10.1016/j.apsusc.2014.08.032>
- [3] Alhulaifi, Abdulaziz S., Gregory A. Buck, and William J. Arbegast. "Numerical and experimental investigation of cold spray gas dynamic effects for polymer coating." *Journal of Thermal Spray Technology* 21, no. 5 (2012): 852-862. <https://doi.org/10.1007/s11666-012-9743-4>
- [4] Srivastava, Anchal, Charudatta Galande, Lijie Ci, Li Song, Chaitra Rai, Deep Jariwala, Kevin F. Kelly, and Pulickel M. Ajayan. "Novel liquid precursor-based facile synthesis of large-area continuous, single, and few-layer graphene films." *Chemistry of Materials* 22, no. 11 (2010): 3457-3461. <https://doi.org/10.1021/cm101027c>
- [5] Shukla, S. K., Swapneel R. Deshpande, Sudheesh K. Shukla, and Ashutosh Tiwari. "Fabrication of a tunable glucose biosensor based on zinc oxide/chitosan-graft-poly (vinyl alcohol) core-shell nanocomposite." *Talanta* 99 (2012): 283-287. <https://doi.org/10.1016/j.talanta.2012.05.052>
- [6] Maarof, Saleha, Amgad Ahmed Ali, and Abdul Manaf Hashim. "Synthesis of large-area single-layer graphene using refined cooking palm oil on copper substrate by spray injector-assisted CVD." *Nanoscale Research Letters* 14, no. 1 (2019): 1-8. <https://doi.org/10.1186/s11671-019-2976-0>
- [7] Zhang, Chuanfang John, and Valeria Nicolosi. "Graphene and MXene-based transparent conductive electrodes and supercapacitors." *Energy Storage Materials* 16 (2019): 102-125. <https://doi.org/10.1016/j.ensm.2018.05.003>
- [8] Szuromi, Phil. "Coat, dope, peel." *Science* 373, no. 6553 (2021): 406-407. <https://doi.org/10.1126/science.373.6553.406-f>
- [9] Zhu, Guoxiang, Wei Zhu, Yang Lou, Jun Ma, Wenqing Yao, Ruilong Zong, and Yongfa Zhu. "Encapsulate α -MnO₂ nanofiber within graphene layer to tune surface electronic structure for efficient ozone decomposition." *Nature Communications* 12, no. 1 (2021): 1-10. <https://doi.org/10.1038/s41467-021-24424-x>
- [10] Salleh, Roszaini Md, Wei-Ming Yeoh, Abdul Rahman Mohamed, and Raihana Bahru. "Effect of Nickel Catalyst Layer Thickness and Grain Size Prepared by Electroplating Method to the Growth of Carbon Nanostructures by Chemical Vapour Deposition." *Sains Malaysiana* 47, no. 2 (2018): 393-402.
- [11] Firdaus, Rabita, Nur Syahidah Afandi, Mehrnoush Khavarian, and Abdul Rahman Mohamed. "Effect of Reaction Time and Catalyst Feed Rate towards Carbon Nanotubes Yields and Purity by Using Rotary Reactor." *Sains Malaysiana* 48, no. 6 (2019): 1187-1194. <https://doi.org/10.17576/jsm-2019-4806-05>
- [12] Hussin, Mohd Rofei Mat, Muhammad Mahyiddin Ramli, Sharaifah Kamariah Wan Sabli, Iskhandar Md Nasir, Mohd Ismahadi Syono, H. Y. Wong, and Mukter Zaman. "Fabrication and characterization of graphene-on-silicon Schottky diode for advanced power electronic design." *Sains Malaysiana* 46, no. 7 (2017): 1147-1154. <https://doi.org/10.17576/jsm-2017-4607-18>
- [13] Shi, Junmei, Pablo Lopez Aguado, Nouredine Guerrassi, and Gavin Dober. "Understanding high-pressure injection primary breakup by using large eddy simulation and x-ray spray imaging." *MTZ Worldwide* 78, no. 5 (2017): 50-57. <https://doi.org/10.1007/s38313-017-0039-4>
- [14] Ortloff, Charles R., and Marlin Vogel. "Spray cooling heat transfer-Test and CFD analysis." In *2011 27th Annual IEEE Semiconductor Thermal Measurement and Management Symposium*, pp. 245-252. IEEE, 2011. <https://doi.org/10.1109/STHERM.2011.5767208>

- [15] Zulkurnai, Fatin Farhanah, Norhidayah Mat Taib, Wan Mohd Faizal Wan Mahmood, and Mohd Radzi Abu Mansor. "Combustion Characteristics of Diesel and Ethanol Fuel in Reactivity Controlled Compression Ignition Engine." *Journal of Advanced Research in Numerical Heat Transfer* 2, no. 1 (2020): 1-13.
- [16] Assael, Marc J., E. A. Sykioti, Marcia L. Huber, and Richard A. Perkins. "Reference Correlation of the Thermal Conductivity of Ethanol from the Triple Point to 600 K and up to 245 MPa." *Journal of Physical and Chemical Reference Data* 42, no. 2 (2013): 023102. <https://doi.org/10.1063/1.4797368>
- [17] Jumadi, Rozita, Amir Khalid, Norrizam Jaat, Iqbal Shahridzuan Abdullah, Nofrizalidris Darlis, Bukhari Manshoor, Azahari Razali, Azwan Sapit, and Ridwan Saputra Nursal. "Analysis of Spray Characteristics and High Ambient Pressure in Gasoline Direct Injection using Computational Fluid Dynamics." *CFD Letters* 12, no. 5 (2020): 36-51. <https://doi.org/10.37934/cfdl.12.5.3651>
- [18] Chishty, Muhammad Aqib, Michele Bolla, Evatt Hawkes, Yuanjiang Pei, and Sanghoon Kook. "Assessing the importance of radiative heat transfer for ECN Spray A using the transported PDF method." *SAE International Journal of Fuels and Lubricants* 9, no. 1 (2016): 100-107. <https://doi.org/10.4271/2016-01-0857>
- [19] Bolla, Michele, Muhammad Aqib Chishty, Evatt R. Hawkes, and Sanghoon Kook. "Modeling combustion under engine combustion network Spray A conditions with multiple injections using the transported probability density function method." *International Journal of Engine Research* 18, no. 1-2 (2017): 6-14. <https://doi.org/10.1177/1468087416689174>